Optimization of a Dihydropyrrolopyrazole Series of Transforming Growth Factor-β Type I Receptor Kinase Domain Inhibitors: Discovery of an Orally Bioavailable Transforming Growth Factor-β Receptor Type I Inhibitor as Antitumor Agent

Hong-yu Li,*[,‡] William T. McMillen,[‡] Charles R. Heap,[▽] Denis J. McCann,[§] Lei Yan,[△] Robert M. Campbell,[⊥] Sreenivasa R. Mundla,[†,#] Chi-Hsin R. King,[▽] Elizabeth A. Dierks,[§] Bryan D. Anderson,[⊥] Karen S. Britt,[⊥] Karen L. Huss,[⊥] Matthew D. Voss,[#] Yan Wang,[‡] David K. Clawson,[‡] Jonathan M. Yingling,[△] and J. Scott Sawyer[‡]

Discovery Chemistry Research and Technology, Drug Disposition Research, Cancer Research, Lead Optimization Biology, and Chemical Product Research and Development, Lilly Research Laboratories, A Division of Eli Lilly and Company, Lilly Corporate Center, Indianapolis, Indiana 46285, and Medicinal Chemistry Department, Albany Molecular Research, Inc., Post Office Box 15098, Albany, New York 12212

Received September 24, 2007

In our continuing effort to expand the SAR of the quinoline domain of dihydropyrrolopyrazole series, we have discovered compound **15d**, which demonstrated the antitumor efficacy with oral bioavailability. This effort also demonstrated that the PK/PD in vivo target inhibition paradigm is an effective approach to assess potential for antitumor efficacy. The dihydropyrrolopyrazole inhibitor **15d** (LY2109761) is representative of a novel series of antitumor agents.

Introduction

Cancer is currently second only to heart disease as a cause of death and will become the primary cause in the next 10 to 20 years.[1] Traditional cancer therapies make use of chemotherapy at the maximum tolerated dose, generally resulting in significant toxicities and often with limited success. The so-called "targeted therapies", such as Gefitinib or Imatinib, are considered less toxic and provide further ammunition in the fight against cancer but often produce responses in only a limited number of cancer patients. New, more universal, more effective, and less toxic therapeutic modalities are therefore desirable.[2]

Angiogenesis plays an important role in the growth of most solid tumors and progression to metastasis.[3] Recently, it has been reported that the specific inhibition of tumor-induced angiogenesis suppresses the growth of many types of solid tumors. For this reason, it is conjectured that the inhibition of angiogenesis represents a novel therapeutic approach against tumors.[4–7] The transforming growth factor-β (TGF-β[a]) type I receptor is a member of a large family of growth factors involved in the regulation of a diverse array of angiogenetic processes. The role of TGF-β in cancer angiogenesis biology is complex and involves aspects of tumor suppression as well as tumor promotion.[8] The ability of TGF-β to potentially inhibit the proliferation of epithelial, endothelial, and hematopoietic cell lineages is central to the tumor suppressing mechanism.[8–12] Therefore, this pathway presents an attractive target for the development of cancer therapeutics that simultaneously attack the tumor and its microenvironment.

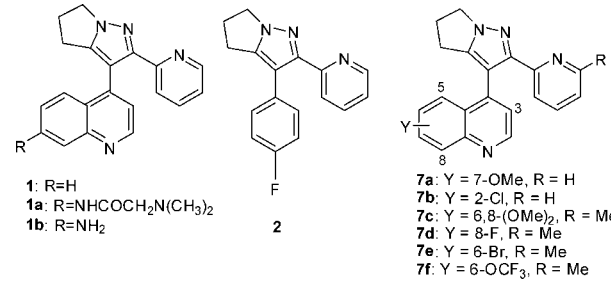

Figure 1

Over the past decade, the pursuit of TGF-β RI kinase small molecule inhibitors has received a high level of attention in the pharmaceutical industry and in the medicinal chemistry community.[13–23] A unique combination of high-throughput screening (HTS), X-ray crystal analysis of TGF-β inhibitors bound to the active site, and structure–activity relationship (SAR) studies has contributed to the discovery of some of the more potent TGF-β RI inhibitors.[17,18] Recently, we reported on the discovery of a new class of small-molecule TGF-β RI inhibitors, the dihydropyrrolopyrazoles, exemplified by compounds **1** and **2** (Figure 1).[17] Although potent TGF-β RI inhibitors were identified and the solubility was improved with the attachment of a solubilizing group through an amine linkage, we found later that representative compound **1a**[17] did not exhibit acceptable PK properties (rat, 10 mg/kg, p.o.; Auc, 398 ng·hr/mL). Moreover, a mini-Ames test on suspected metabolite **1b** (also a potent TGF-β RI inhibitor) was positive, indicating a likelihood of mutagenicity. During the continuing SAR effort around quinoline ring substitutions, we have discovered that after replacing the amine linker with an ether linkage, the oral

* Corresponding author. Phone: 317-433-3349. Fax: 317-276-7600. e-mail: li_hong-yu@lilly.com.

‡ Discovery Chemistry Research and Technology, Lilly Research Laboratories.

▽ Albany Molecular Research, Inc.

§ Drug Disposition Research, Lilly Research Laboratories.

△ Cancer Research, Lilly Research Laboratories.

⊥ Lead Optimization Biology, Lilly Research Laboratories.

† Present Address: sreeni@sreenilabs.com. Sreeni Labs Private Limited, Flat No. 504, Vijayasree Apartments, Behind Chermas, Ameerpet, Hyderabad 500 073, A.P., India.

Chemical Product Research and Development, Lilly Research Laboratories.

[a] Abbreviations: TGF-β, transforming growth factor-β; TGF-β RI, transforming growth factor-β type I receptor; HTS, high-throughput screening; IVTI, in vivo target inhibition; BID, twice daily; Smad, a composite term derived from *Sma* genes from *Caenorhabditis elegans* and *Mad* gene (*Drosophila melanogaster*) involved as intracellular substrate for TGF-β and BMP signaling; Lck, leukocyte-specific protein tyrosine kinase; Sapk, stress-activated protein kinase; MKK, mitogen-activated protein kinase kinase; Fyn, a molecule, present in the signaling pathway of integrins; JNK, c-Jun N-terminal kinase.

10.1021/jm701199p CCC: $40.75
Published on Web 03/04/2008

Scheme 1[a]

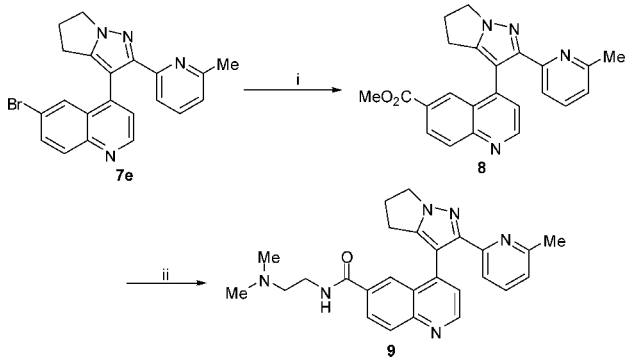

[a] Reagents and conditions: (i) CO, $Pd(OAc)_2$, PPh_3, NaOAc, DMF/MeOH, 80 °C, 66%; (ii) $(Me)_2NCH_2CH_2NH_2$, 100 °C, 74%.

Scheme 2[a]

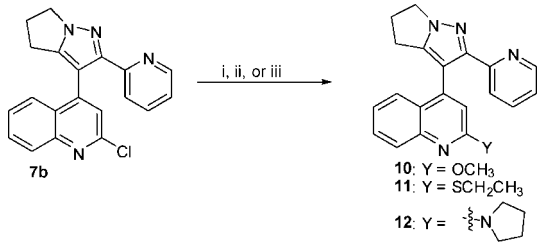

[a] Reagents and conditions: (i) for **10**: NaH, MeOH, 0 to 50 °C, 96 h, 88%; (ii) for **11**: NaH, EtSH DMF, 0 °C to RT, 72 h, 87%; (iii) for **12**: pyrrolidine, 80 °C, 96 h, 91%.

exposure in rat was improved. Subsequently, activity in both in vivo target inhibition (IVTI) and xenograft efficacy models was demonstrated. In this paper, we report the discovery and SAR of small molecule **15d**, which demonstrated oral antitumor efficacy.

Chemistry

The construction of the dihydropyrrolopyrazole ring with differentially substituted quinolines by following procedures published previously (**7a**−**7f**, Figure 1)[17] is shown in Supporting Information.

Methyl benzoate **8** and amide analogue **9** were derived from compound **7e**, as depicted in Scheme 1. Palladium-catalyzed carbonylation of bromide **7e** with carbon monoxide in the presence of $Pd(OAc)_2$, PPh_3, and NaOAc in DMF/MeOH gave methyl benzoate **8**. The ester structural moiety was then treated with 2-*N*,*N*-dimethylaminoethylamine neat at 100 °C to afford amide **9**. The derivatization at the 2-position of the quinoline is outlined in Scheme 2. The heating of chloride **7b** in MeOH or pyrrolidine gave compound **10** or **12**, respectively. In the case of the synthesis of compound **10**, NaH was required. Similarly, compound **11** was synthesized with EtSH in DMF catalyzed by NaH.

Substitutions at the 7-position of the quinoline moiety are shown in Schemes 3 and 4. Demethylation of the methoxy group in compound **7a** went smoothly with HBr and produced compound **13** in 99% yield. Alkylation of phenol **13** catalyzed by Cs_2CO_3 was straightforward (yields ∼ 15–70%), except for compound **15**. Due to the β-elimination of 1-bromo-2-chloroethane (see Supporting Information), the yield for the synthesis of compound **15** was low (six conditions, ∼10%) and purification was not synthetically practical. However, by using the corresponding mesylate instead of the bromide, alkylation went well in 45% yield. The transformation of ester **17** to amide **17a**

Scheme 3[a]

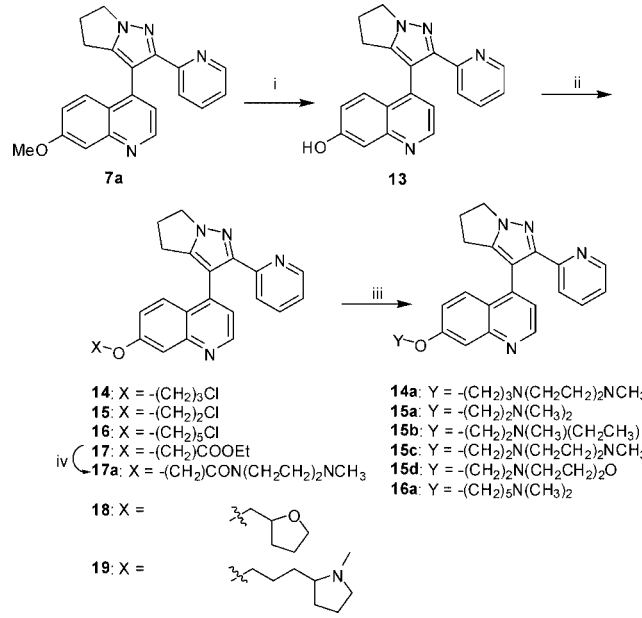

[a] Reagents and conditions: (i) HBr, 99%; (ii) bromide/or mesylate, Cs_2CO_3, for **14**, 79%; for **15**, 46%; for **16**, 79%; for **17**, 39%; for **18**, 15%; for **19**, 35%; (iii) amine, DMF, for **14a**, 75%; for **15a**, 93%; for **15b**, 64%; for **15c**, 71%; for **15d**, 65%; for **16a**, 49%; (iv) (a) LiOH/MeOH; (b) $COCl_2$; (c) *N*-Me-piperazine (overall yield, 48% for **17a**).

Scheme 4[a]

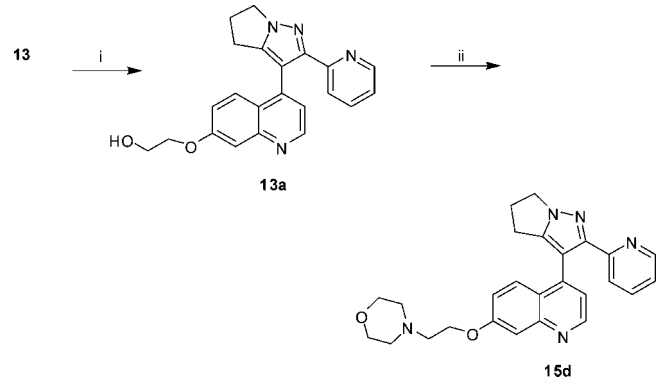

[a] Reagents and conditions: (i) (a) 2-(2-bromoethoxy)tetrahydro-2*H*-pyran, Cs_2CO_3, DMF; (b) AcOH, THF, H_2O; (ii) (a) MsCl, pyr; (b) morpholine; for four steps, 81%.

proceeded in moderate yield (48%) via hydrolysis and conversion to the acyl chloride, followed by treatment with *N*-methylpiperazine. The reaction of chlorides **14**−**16**, either neat or in DMF with various amines, furnished the final compounds (**14a**, **15a**−**d**, and **16a**). Alternatively, the alcohol was synthesized in a two-step sequence via alkylation with 2-bromoethoxy-THP followed by deprotection of the THP group with AcOH. Mesylation of the alcohol followed by displacement using the appropriate amine quantitatively afforded compound **15d** (Scheme 4).

To explore the SAR at the 7-position of the quinoline ring, the electron-deficient substrate 4-fluorobenzonitrile was reacted with phenol **13** in the presence of 37% KF on alumina.[24] This reaction provided a 95% yield of the desired product **20a** along with 4% of amide **20b** derived from the further hydrolysis of **20a** (Scheme 5). Hydrolysis of nitrile **20a** with HCl followed by acid chloride formation and treatment with dimethyl amine gave dimethylamide **22**. Conversion of the amide to thioamide with Lawesson reagent was followed by treatment with hydra-

Scheme 5[a]

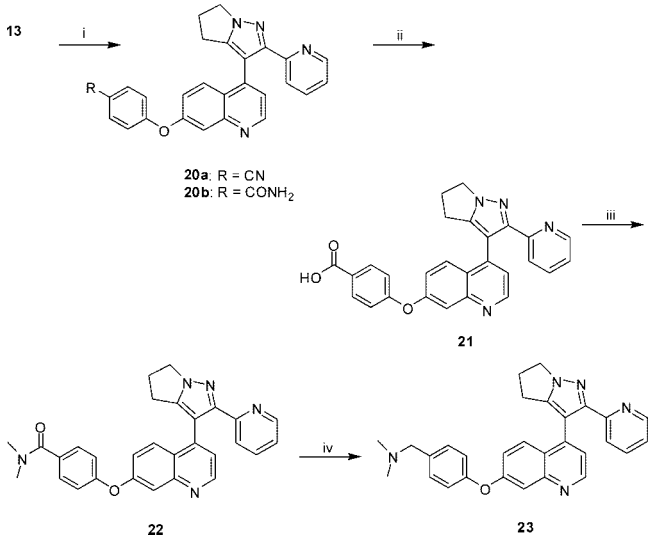

[a] Reagents and conditions: (i) 4-fluorobenzonitrile, 18-crown-6, 37% KF on alumina, DMF, for **20a**, 95%; for **20b**, 4%; (ii) HCl, 100%; (iii) (a) ClCOCOCl, CH_2Cl_2; (b) dimethylamine in THF, 54%; (iv) (a) Lawesson's reagent, toluene; (b) NH_2NH_2, Raney nickel, MeOH, refluxed, 20%.

zine and Raney nickel. Final compound **23** was purified by the combination of normal phase and reverse-phase chromatography.

Results and Discussion

Although some of the SAR on the 7-position of the quinoline has been reported,[17,18] a detailed study of ether-linked side-chains provided an opportunity for the further optimization of physical properties and, subsequently, for in vivo activity. The medicinal chemistry effort was initially focused on evaluating the effect of substitutions in both biochemical and cellular assays. LY364947 (4-[3-(pyridin-2-yl)-1*H*-pyrazol-4-yl]-quinoline)[16] was used as a standard compound for calibration of assay results. As we investigated the substituent requirement at the 2-position of quinoline, we found that chloride, along with various other groups (-OMe, -SEt, and -pyrrolidine), exhibited very weak activity with IC_{50} value >20 μM (Table 1). However, substitution at the 6-position produced more active compounds. Interestingly, both electron-deficient and relatively small groups were tolerated at the 6-position and gave potent activities in both the enzymatic assay (IC_{50} ~100 nM) and cell-based assays (IC_{50} 50–300 nM). Substitutions through an ester or amide combined with a solubilizing tail were detrimental. Compound **7f** (6-OCF_3) gave IC_{50} values of ~0.2 μM in both cell-based assays, while compound **9** (6-$CONH(CH_2)_2N(CH_3)_3$) gave an IC_{50} of only 2.27 μM in the NIH 3T3 cell-proliferative assay. Substitution at the 8-position with fluorine to give **7d** substantially diminished in vitro activity. Double substitutions at the 6- and 8-positions with methoxy further supported the observation that groups at the 8-position are not well tolerated (Table 1).

It was reported that compounds with substituents at the 7-position comprised of electron-donating groups overall gave good activity in vitro.[17,18] Further expansion of the SAR at the 7-position using novel aminoalkoxy side chains (**14**–**19**) gave very potent inhibitors in the TGF-β RI assay with IC_{50} values ranging from 6 to 129 nM. In contrast, the IC_{50} values of compounds with phenyloxy side chains (**20**–**23**) were only 748–4820 nM, ~100-fold less potent. Although the X-ray crystal structure of **15d** showed that the solubilizing group orients toward solvent (Figure 2), the phenyl ether linker of compound **23** is apparently too large for extension of the amine tail completely into solvent. In addition, the solvation effect on potency was also evident because compounds with basic amines at the terminal position of the side chain gave slightly higher activity in comparison with other substituted analogues (Table 1).

Inhibitors were then run through a diverse kinase panel to examine selectivity profiles. Inhibitors **15a** and **15d** were highly selective against ~50 kinases, although weak activities were observed for Lck, Sapk2α (p38α-MAPK), MKK6, Fyn, and JNK3 (18–89% inhibition at the 20 μM, see Supporting Information).

Compounds that showed cell-based activities under ~0.2 μM were evaluated for metabolism in vitro. Compounds bearing a basic amine group at the terminal end of the side chains (**14a**, **15a**, **15b**, and **15d**) have generally moderate to low metabolism levels (<60% in both rat and human microsomes), indicating that they are more likely to give adequate in vivo exposure (see Supporting Information). Compound **15d** was subjected to a rat exposure study (10 mg/kg oral) and good exposure (Auc $\approx$ 1000 ng·hr/mL, 24 h) was observed. Importantly, acceptable bioavailability (*F*, 21%, compound **15d**) was also achieved.

An IVTI assay based on inhibition of pSmad2 was performed using three different protocols: single point screening at 50 mg/kg oral, pharmacokinetic (PK) studies at multiple doses for compounds having passed a 50% threshold target inhibition at 50 mg/kg oral, and a time-course pharmacodynamic (PD) study at 75 mg/kg oral. In the event, all compounds that showed less metabolism in vitro achieved more than 50% target inhibition in vivo. This further confirmed that metabolism surrogates provided useful and reliable data for predicting IVTI activity. In the PK studies, the ED_{50} was analyzed as inhibition versus plasma concentration (Supporting Information). As a result, compound **15d** was identified as the most potent TGF-β RI inhibitor in vivo with an EC_{50} value of 0.268 μM. Inhibition during the time-course experiment of optimal compound **15d** was measured at 0.5, 1, 2, 4, 8, and 24 h data points. As expected, long duration of target inhibition (~50% inhibition after 4 h) was observed and correlated well with plasma concentrations (Supporting Information).

Evaluation of efficacy was then performed in a nude mouse tumor growth xenograft model bearing the human MX1-breast carcinoma that has previously been demonstrated to be sensitive to TGF-β inhibition. Compound **15d** was administrated BID via oral gavage in a saline solution starting on day 7 postimplantation and continued for 20 days. Tumors were allowed to grow to a size of 2500 cm^3 prior to study termination. Analysis of the PK/PD data of compound **15d** indicated that a dose of 75 mg/kg BID should be sufficient, and at this dose, a statistically significant tumor growth delay in the MX1 model was observed (Figure 3). No body weight loss was observed in most of the treatment groups.

In conclusion, our expanded series of TGF-β RI inhibitors has demonstrated antitumor efficacy and represents novel antitumor agents. Traditional medicinal chemistry techniques were used to quickly delineate the SAR of compounds having new substitution on the quinoline ring. At the quinoline 6-position, small substituents were tolerated, while large substitutions diminished the potency significantly. Although substitution at the 7-position with a bulky phenoxy group was detrimental, incorporating a basic amine side-chain through an ether linkage was not only tolerable, but also provided compounds with oral bioavailability such as **15d**. The surrogate

Table 1. Kinase and Cellular Activity[a]

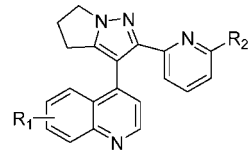

compounds	R1	R2	TGF-β R1 IC_{50}, μM	p3TP-Lux IC_{50}, μM	NIH 3T3 IC_{50}, μM
LY364947	See ref. 17	H	0.059 ± 0.023	0.04 ± 0.022	0.081 ± 0.067
7b	2-Cl	H	19.8 ± 0.2 (2)	>20	>20
7c	6,8-OMe	Me	3.81	7.20	>20
7d	8-F	Me	0.928 ± 0.296 (2)	0.951 ± 0.218 (3)	1.03 ± 0.665 (2)
7e	6-Br	Me	0.089 ± 0.022 (2)	0.055 ± 0.0030 (2)	0.338 ± 0.156 (2)
7f	6-OCF_3	Me	0.141 ± 0.042 (2)	0.201 ± 0.0010 (2)	0.254
8	6-COOMe	Me	0.526	0.403	NT
9	6-$CONH(CH_2)_2N(CH_3)_3$	Me	0.193	0.468 ± 0.212 (3)	2.27 ± 0.334 (4)
10	2-OMe	H	>20	NT	NT
11	2-SEt	H	>20	>20	NT
12	2-$N(CH_2)_4$	H	>20	>20	NT
13	7-OH	H	0.16	0.20 ± 0.073 (2)	0.42 ± 0.41 (2)
14a	7-$O(CH_2)_3N(CH_2CH_2)_2NCH_3$	H	0.074	0.044 ± 0.042 (4)	0.092 ± 0.054 (4)
15	7-$O(CH_2)_2Cl$	H	0.033	0.066 ± 0.054 (2)	0.097 ± 0.047 (3)
15a	7-$O(CH_2)_2N(CH_3)_2$	H	0.024 ± 0.010 (2)	0.029 ± 0.010 (7)	0.098 ± 0.077 (9)
15b	7-$O(CH_2)_2N(CH_2CH_3)(CH_3)$	H	0.085 ± 0.051 (2)	0.061 ± 0.030 (5)	0.072 ± 0.027 (7)
15c	7-$O(CH_2)_2N(CH_2CH_2)_2NCH_3$	H	0.10 ± 0.071 (3)	0.038 ± 0.012 (3)	0.054 ± 0.032 (4)
15d	7-$O(CH_2)_2N(CH_2CH_2)_2O$	H	0.069 ± 0.031 (2)	0.18 ± 0.093 (5)	0.21 ± 0.17 (4)
16a	-$(CH_2)_5N(CH_3)_2$	H	0.047	0.024 ± 0.0080 (3)	0.051 ± 0.018 (3)
17a	7-$OCH_2CON(CH_2CH_2)_2NCH_3$	H	0.049	0.26 ± 0.16 (2)	0.73 ± 0.22 (2)
18	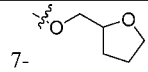	H	0.13	0.080 ± 0.012 (3)	0.25 ± 0.10 (3)
19	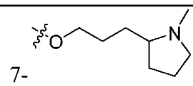	H	0.072 ± 0.053 (5)	0.017 ± 0.0010 (3)	0.020 ± 0.010 (3)
20a	7-OPh-*p*-CN	H	1.2 ± 0.61 (6)	NT	NT
20b	7-OPh-*p*-$CONH_2$	H	1.1	NT	NT
21	7-OPh-*p*-COOH	H	4.8 ± 3.3 (6)	>20 (2)	>20 (2)
22	7-OPh-*p*-$CON(CH_3)_2$	H	1.1 ± 0.66 (6)	15 ± 0 (2)	5.1 ± 0.038 (2)
23	7-OPh-*p*-$CH_2N(CH_3)_2$	H	0.75	NT	NT

[a] All IC_{50} values were 10 point determinations. Mean values ± SEM for a minimum of two determinations.

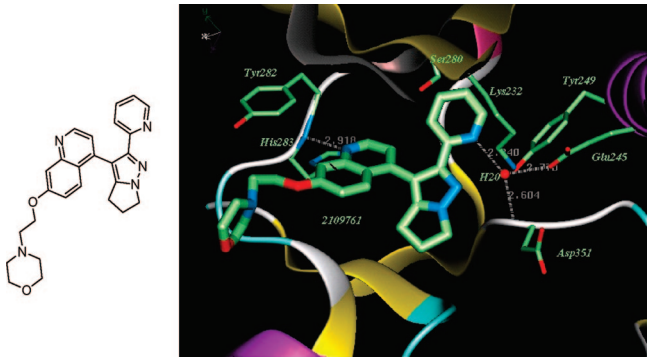

Figure 2. X-ray crystal structure of **15d** bound to the ATP binding site of the TGF-β R1 kinase domain. The structure indicates the basic amine tail orients outside of the binding pocket and within the solvent.

metabolism SAR was implemented to predict/select compounds with better metabolism properties in vitro and helped to rapidly identify appropriate compounds for testing in in vivo PK/PD IVTI assays. A hallmark of this effort was also the successful use of the PK/PD data to design long-term tumor xenograft efficacy studies.

Experimental Section

3-[6-(2-Morpholin-4-yl-ethoxy)-naphthalen-1-yl]-2-pyridin-2-yl-5,6-dihydro-4*H*-pyrrolo[1,2-*b*]pyrazole (15d). To a solution of phenol (**13**, 376 mg, 1.15 mmol) and cesium carbonate (826 mg, 2.54 mmol) in DMF (5 mL) was added 2-(2-bromoehtoxy)tetrahydro-2*H*-pyran (380 μL, 2.52 mmol). The resulting content was stirred at 120 °C for 4 h, quenched with saturated sodium chloride, and then extracted with chloroform. The organic layer was dried over sodium sulfate and concentrated in vacuo. The residue was purified by silica gel column chromatography (linear gradient from dichloromethane to 10% methanol/dichloromethane over 20 min and 10% methanol/dichloromethane for 20 min) to give a yellow oil (424 mg). LRMS (ES^+) *m/z* 457.0 $(M + 1)^+$.

To a solution of AcOH/THF/H_2O (4:2:1; 20 mL) was added THP (tetrahydro-2*H*-pyran)-protected compound (421 mg, 0.92 mmol). After stirring at 80 °C overnight, solvent was removed in vacuo. The residue was dissolved in $CHCl_3$/*i*-PrOH (3:1) and washed with saturated Na_2SO_4. The organic layer was dried over sodium sulfate and concentrated in vacuo. The resulting foam (**13a**) was pure enough without further purification (425 mg). LRMS (ES^+) *m/z* 373.1 $(M + 1)^+$.

To a solution of alcohol (**13a**, 293 mg, 0.78 mmol) in dried pyridine (5 mL) was added $MeSO_2Cl$ (68 μL, 0.81 mmol). After stirring for 2 h, pyridine was removed in vacuo. The residue was dissolved in $CHCl_3$ and washed with saturated $NaHCO_3$. The

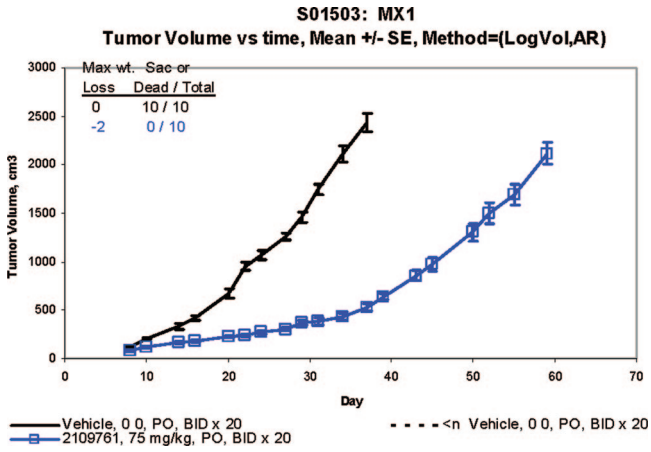

Figure 3. Effect of **15d** (LY2109761) on the growth of the MX1 human breast cancer cell line in nude mice. Cells were implanted into a group of 10 Charles River nude mice at 10^6 cells subcutaneously. Compound **15d** was administrated by BID oral gavage starting on day 7 (<100 cm^3) and continued for 20 days. Tumors were allowed to grow until a size of 2500 cm^3 prior to study termination. Tumor volume data were transformed to a log scale for analysis to equalize variance across time and treatment groups. SAS PROC MIXED was used separately for each treatment group with AR (1) autocorrelation to calculate and plot adjusted means and standard errors at each time point. Tumor growth delay was calculated as the difference in time to reach 1000 cm^3 between treated and control groups.

organic layer was dried over Na_2SO_4 to give a pure white foam without further purification (425 mg). LRMS (ES^+) *m/z* 451.1 $(M + 1)^+$.

A solution of mesylate (87 mg, 0.19 mmol) in morpholine (1 mL) was stirred at 50 °C for 4 h. After morpholine was removed in vacuo, the crude product was dissolved in *i*-PrOH/$CHCl_3$ (1:3) and washed with sodium chloride. The organic layer was dried over Na_2SO_4 and concentrated in vacuo to give a pure slight yellow solid (**15d**, 83 mg, 81% overall yield for four steps). LRMS (ES^+) *m/z* 442.0 $(M + 1)^+$. HRMS (AP^+) calcd for $C_{26}H_{27}N_5O_2$, 441.2165; found, 441.2158. HPLC (system C), >99% ($t_R = 0.45$ min); (system D), 97% ($t_R = 2.37$ min).

Acknowledgment. We are grateful to Dr. Philip W. Iversen and Mr. Jason R. Manro for their statistical contributions and suggestions.

Supporting Information Available: General experimental procedure and procedures for preparation of **7c–7f**, **8–13**, **14a**, **15**, **15a–c**, **16a**, **17a**, **18–19**, **20a**,**b**, **21–23**, and their precursors; NMR data of **13a** and **15d**. Scheme for synthesis of **7a–f**; Enzymatic and cell-based assay procedures; IVTI PK and PD data for key compounds; Kinase selectivity (**15d**); Table for screening of alkylation condition of phenol **13**; ADME surrogate data for key compounds; HPLC purities of all target compounds, and HPLC tracings of **15d**. This material is available free of charge via the Internet at http://pubs.acs.org.

References

(1) *Cancer Facts and Figures, 2004*, American Cancer Society, Inc., **2004**; p 5, www.cancer.org.
(2) Donate, F. Antiangiogenic therapy in cancer. *Drugs Future* **2005**, *30*, 695–706.
(3) Folkman, J. Anti-angiogenesis: New concept for therapy of solid tumors. *Ann. Surg.* **1972**, *175*, 409–416.
(4) Liotta, L. A.; Kleinerman, J.; Saidel, G. M. Quantitative relationships of intravascular tumor cells, tumor vessels, and pulmonary metastases following tumor implantation. *Cancer Res.* **1974**, *34*, 997–1004.
(5) Eckhardt, S. G. Angiogenesis Inhibitors as Cancer Therapy. *Hosp. Pract.* **1999**, *284*, 808–812.
(6) Bergers, G.; Javagerian, K.; Lo, K.-M.; Folkman, J.; Hanahan, D. Effects of angiogenesis inhibitors on multistage carcinogenesis in mice. *Science* **1999**, *284*, 808–812.
(7) Fan, T.-P. D.; Jaggar, R.; Bicknell, R. Controlling the vasculature: Angiogenesis, anti-angiogenesis and vascular targeting of gene therapy. *Trends Pharmacol. Sci.* **1995**, *16*, 57–66.
(8) Yingling, J. M.; Blanchard, K. L.; Sawyer, J. S. Development of TGF-β signaling inhibitors for cancer therapy. *Nat. Rev. Drug Discovery* **2004**, *3*, 1011–1022.
(9) Akhurst, R. J.; Derynk, R. TGF-β signaling in cancer—A double-edged sword. *Trends Cell Biol.* **2001**, *11* (11), S44–S51.
(10) Derynk, R.; Akhurst, R. J.; Balmain, A. TGF-β signaling in tumor suppression and cancer progression. *Nat. Genet.* **2001**, *29*, 117–129.
(11) Massague, J.; Blain, S. W.; Lo, R. S. TGF-β signaling in growth control, cancer, and heritable disorders. *Cell* **2000**, *103*, 295–309.
(12) de Caestecker, M. P.; Piek, E.; Roberts, A. B. Role of transforming growth factor-β signaling in cancer. *J. Nat. Cancer Inst.* **2000**, *92* (17), 1388–1402.
(13) Callahan, J. F.; Burgess, J. L.; Fornwald, J. A.; Gaster, L. M.; Harling, J. D.; Harrington, F. P.; Heer, J.; Kwon, C.; Lehr, R.; Mather, A.; Olson, B. A.; Weinstock, J.; Laping, N. J. Identification of novel inhibitors of the transforming growth factor β1 (TGF-β1) type I receptor (ALK5). *J. Med. Chem.* **2002**, *45*, 999–1001.
(14) Laping, N. J.; Grygielko, A.; Mathur, A.; Butter, S.; Bomberger, J.; Tweed, C.; Martin, W.; Fornwald, J.; Lehr, R.; Harling, J.; Gaster, J. F.; Olson, B. A. Inhibition of transforming growth factor (TGF)-β1-induced extracellular matrix with a novel inhibitor of the TGF-β type I receptor kinase activity: SB-431542. *Mol. Pharmacol.* **2002**, *62* (1), 58–64.
(15) Inman, G. J.; Nicolas, F. J.; Callahan, J. F.; Harling, J. D.; Gaster, L. M.; Reith, A. D.; Laping, N. J.; Hill, C. S. SB-431542 is a potent and specific inhibitor of transforming growth factor-β superfamily type I activin receptor-like kinase (ALK) receptors ALK4, ALK5, and ALK7. *Mol. Pharmacol.* **2002**, *62* (1), 65–74.
(16) Sawyer, J. S.; Anderson, B. D.; Beight, D. W.; Campbell, R. M.; Jones, M. L.; Herron, D. K.; Lampe, J. W.; McCowan, J. R.; McMillen, W. T.; Mort, N.; Parsons, S.; Smith, E. C. R.; Vieth, M.; Weir, L. C.; Yan, L.; Zhang, F.; Yingling, J. M. Synthesis and activity of new aryl- and heteroaryl-substituted pyrazole inhibitors of the transforming growth factor-β type 1 receptor kinase domain. *J. Med. Chem.* **2003**, *46*, 3953–3956.
(17) Sawyer, J. S.; Anderson, B. D.; Beight, D. W.; Goodson, T.; Herron, D. K.; Li, H.-Y.; McMillen, W. T.; Mort, N.; Parsons, S.; Smith, E. C. R.; Britt, K. S.; Yan, L.; Zhang, F.; Yingling, J. M. Synthesis and activity of new aryl- and heteroaryl-substituted 5,6-dihydro-4*H*-pyrrolo[1,2-*b*]pyrazole inhibitors of the transforming growth factor-β type I receptor kinase domain. *Bioorg. Med. Chem. Lett.* **2004**, *14*, 3581–3585.
(18) Li, H.-Y.; Wang, Y.; Yan, L.; Campbell, R. M.; Anderson, B. D.; Wagner, J. R.; Yingling, J. M. Novel and potent transforming growth factor beta type I receptor kinase domain inhibitor: 7-Amino 4-(2-yl-5,6-dihydro-4*H*-pyrrolo[1,2-*b*]pyrazol-3-yl)-quinoline. *Bioorg. Med. Chem. Lett.* **2004**, *14*, 3585–3588.
(19) Singh, J.; Ling, L. E.; Sawyer, J. S.; Lee, W. C.; Zhang, F.; Yingling, J. M. Transforming the TGFβ pathway: Convergence of distinct lead generation strategies on a novel kinase pharmacophore for TβR1 (ALK5). *Curr. Opin. Drug Discovery Dev.* **2004**, *7*, 437–445.
(20) Gellibert, F.; Woolven, J.; Fouchet, M.-H.; Mathews, N.; Goodland, H.; Lovegrove, V.; Laroze, A.; Nguyen, V.-L.; Sautet, S.; Wang, R.; Janson, C.; Smith, W.; Krysa, G.; Boullay, V.; de Gouville, A.-C.; Huet, H.; Hartley, D. Identification of 1,5-naphthyridine derivatives as a novel series of potent and selective TGF-β type I receptor inhibitors. *J. Med. Chem.* **2004**, *47*, 4494–4506.
(21) Li, H.-Y.; Wang, Y.; Heap, C. R.; King, C.-H. R.; Mundla, S. R.; Voss, M.; Clawson, D. K.; Yan, L.; Campbell, R. M.; Anderson, B. D.; Wagner, J. R.; Britt, K.; Lu, K. X.; McMillen, W. T.; Yingling, J. M. Dihydropyrrolopyrazole transforming growth factor-β type I receptor kinase domain inhibitors: A novel benzimidazole series with selectivity versus transforming growth factor-β type II receptor kinase and mixed lineage kinase-7. *J. Med. Chem.* **2006**, *49*, 2138–2143.
(22) Kim, D.-K.; Jang, Y.; Lee, H. S.; Park, H.-J.; Yoo, J. Synthesis and biological evaluation of 4(5)-(6-alkylpyridin-2-yl)imidazoles as transforming growth factor-β type I receptor kinase inhibitors. *J. Med. Chem.* **2007**, *50*, 3143–3147.
(23) Li, H.-Y.; Wang, Y.; McMillen, W. T.; Chatterjee, A.; Toth, J. E.; Mundla, S. R.; Voss, M.; Boyer, R. D.; Sawyer, J. S. A concise synthesis of quinazolinone TGF-β R1 inhibitor through one-pot three-component Suzuki−Miyaura/etherification and imidata-amide rearrangement reactions. *Tetrahedron* **2007**, *63*, 11763–11770.
(24) Sawyer, J. S.; Schmitting, E. A.; Palkowitz, J. A.; Smith, W. J., III. Synthesis of diaryl ethers, diaryl thioethers, and diaryl amines mediated by potassium fluoride-alumina and 18-crown-6: Expansion of scope and utility. *J. Org. Chem.* **1998**, *63*, 6338–6343.

JM701199P